

The Amphoterin (HMGB1)/Receptor for Advanced Glycation End Products (RAGE) Pair Modulates Myoblast Proliferation, Apoptosis, Adhesiveness, Migration, and Invasiveness

FUNCTIONAL INACTIVATION OF RAGE IN L6 MYOBLASTS RESULTS IN TUMOR FORMATION IN VIVO*

Received for publication, August 26, 2005, and in revised form, January 4, 2006. Published, JBC Papers in Press, January 9, 2006, DOI 10.1074/jbc.M509436200

Francesca Riuzzi^{†1}, Guglielmo Sorci^{‡1}, and Rosario Donato^{‡§2}

From the [†]Department of Experimental Medicine and Biochemical Sciences and [§]Istituto Interuniversitario di Miologia, University of Perugia, Casella Postale 81 Succursale 3, 06122 Perugia, Italy

We reported that RAGE (receptor for advanced glycation end products), a multiligand receptor of the immunoglobulin superfamily expressed in myoblasts, when activated by its ligand amphoterin (HMGB1), stimulates rat L6 myoblast differentiation via a Cdc42-Rac-MKK6-p38 mitogen-activated protein kinase pathway, and that RAGE expression in skeletal muscle tissue is developmentally regulated. We show here that inhibition of RAGE function via overexpression of a signaling deficient RAGE mutant (RAGE Δ cyto) results in increased myoblast proliferation, migration, and invasiveness, and decreased apoptosis and adhesiveness, whereas myoblasts overexpressing RAGE behave the opposite, compared with mock-transfected myoblasts. These effects are accompanied by a decreased induction of the proliferation inhibitor, p21^{Waf1}, and increased induction of cyclin D1 and extent of Rb, ERK1/2, and JNK phosphorylation in L6/RAGE Δ cyto myoblasts, the opposite occurring in L6/RAGE myoblasts. Neutralization of culture medium amphoterin negates effects of RAGE activation, suggesting that amphoterin is the RAGE ligand involved in RAGE-dependent effects in myoblasts. Finally, mice injected with L6/RAGE Δ cyto myoblasts develop tumors as opposed to mice injected with L6/RAGE or L6/mock myoblasts that do not. Thus, the amphoterin/RAGE pair stimulates myoblast differentiation by the combined effect of stimulation of differentiation and inhibition of proliferation, and deregulation of RAGE expression in myoblasts might contribute to their neoplastic transformation.

Myogenesis is a multistep process in which the precursors of myofibers, the myoblasts, first proliferate and then differentiate into fusion-competent cells that finally fuse with each other to form myotubes (1–3). A similar process occurs in mature skeletal muscles in case of damage; quiescent, mononucleated cells, the satellite cells, that coexist with myofibers, can be activated by a number of extracellular factors to proliferate and then to differentiate as above to repair the damaged myofibers (3). In both cases, proliferation and differentiation are sepa-

rate and mutually exclusive events that must occur sequentially in that order.

Proliferation arrest is one critical step in the process of embryonic myogenesis and muscle regeneration/repair (3). Either excessive or defective myoblast and satellite cell proliferation can result in altered skeletal muscle formation because myoblasts cannot activate pro-myogenic signaling pathways in the former case, and because of the low density and insufficient cell-cell contacts that hamper myoblast fusion into myotubes in the second case. Thus, embryonic myogenesis and the closely related muscle regeneration appear to be the net result of the action of a cohort of factors that balance each others activities in a timely and highly coordinated manner so as to assure a sized extent of muscle tissue formation. These factors will assure an appropriate extent of myoblast and satellite cell proliferation at sites of skeletal muscle formation during embryogenesis and in damaged muscles, respectively, and/or will trigger the myogenic differentiation program in proliferation-arrested myoblasts and satellite cells. Thus, some of these factors stimulate myoblast proliferation and differentiation (e.g. insulin and insulin-like growth factors and their receptors), other factors promote myoblast fusion into myotubes (e.g. BOC, CDO, neogenin and its ligand, netrin), whereas other factors inhibit myoblast proliferation and differentiation (e.g. tumor necrosis factor- α , transforming growth factor- β , and myostatin), and still other factors (e.g. basic fibroblast growth factor, hepatocyte growth factor and, as recently shown, S100B) stimulate myoblast proliferation and/or modulate myoblast differentiation (3–15).

We have reported that amphoterin (HMGB1) and its receptor for advanced glycation end products (RAGE)³ promote rat L6 myoblast differentiation and myotube formation by up-regulating the expression of the muscle-specific transcription factor, myogenin, via a Rac1-Cdc42-MKK6-p38 MAPK pathway (16). RAGE is a multiligand receptor belonging to the immunoglobulin superfamily that has been implicated in the regulation of several activities/processes such as protection of neurons against stress and stress-induced neuronal death depending on the nature of the ligand and the duration and intensity of its activation, the inflammatory response, tumorigenesis and, as mentioned above, myoblast terminal differentiation (16, 17). Amphoterin (HMGB1), a low molec-

* This work was supported by the Ministero dell'Istruzione, dell'Università e della Ricerca-University of Perugia (PRIN 2004, 2004054293), Fondazione Cassa di Risparmio di Perugia Project 2004.0282.020_001, and the Associazione Italiana per la Ricerca contro il Cancro (AIRC 1110) (to R. D.). The costs of publication of this article were defrayed in part by the payment of page charges. This article must therefore be hereby marked "advertisement" in accordance with 18 U.S.C. Section 1734 solely to indicate this fact.

¹ Both authors contributed equally to this work.

² To whom correspondence should be addressed: Section of Anatomy, University of Perugia, Via del Giochetto C.P. 81 Succ. 3, 06122 Perugia, Italy. Tel.: 39-075-585-7453 or 7448; Fax: 39-075-585-7451; E-mail: donato@unipg.it.

³ The abbreviations used are: RAGE, receptor for advanced glycation end products; DM, differentiation medium; DMEM, Dulbecco's modified Eagle's medium; ERK1/2, extracellular signal-regulated kinases 1/2; FACS, fluorescence-activated cell sorting; FBS, fetal bovine serum; GM, growth medium; JNK, c-Jun NH₂ terminal protein kinase; MAPK, mitogen-activated protein kinase; RAGE Δ cyto, RAGE mutant lacking the cytoplasmic and transducing domain; Rb, retinoblastoma suppressor protein; MMP, matrix metalloproteinase; PBS, phosphate-buffered saline; VCAM, vascular cell adhesion molecule; NCAM, neural cell adhesion molecule.

ular weight protein with both intracellular and extracellular regulatory activities (18), is one established RAGE ligand that is normally found in serum and extracellular fluids (17, 19). Besides stimulating myogenesis *in vitro* via RAGE activation, amphoterin has been shown to promote skeletal muscle repair when administered to dystrophic mice, via stimulation of mesoangioblast homing into the diseased muscle tissue (20), possibly via RAGE binding in the light of our previous data (16).

We found that overexpression of RAGE in L6 myoblasts resulted in a significant extent of myoblast differentiation and fusion into myotube even in growth medium (GM, 10% fetal bovine serum (FBS)) and in an acceleration of differentiation of myoblasts in differentiation medium (DM, 2% FBS), whereas overexpression of a RAGE mutant lacking the cytoplasmic and transducing domain (RAGE Δ cyto) resulted in a reduced tendency of myoblasts in DM to differentiate, compared with wild type and mock-transfected myoblasts (16). Overall, the activation of the MKK6-p38 MAPK signaling pathway for the amphoterin/RAGE pair to promote myoblast differentiation is in line with the notion that p38 MAPK needs to be activated for terminal differentiation to take place (21–24). Specifically, the amphoterin/RAGE pair might be one trigger of the signaling cascade leading to p38 MAPK activation in differentiating myoblasts.

In the present study we addressed the question whether RAGE engagement in myoblasts and the resulting p38 MAPK activation might determine changes in myoblast proliferation as well as other processes such as apoptosis, adhesiveness, migration, and invasiveness, which characterize myoblast terminal differentiation and fusion into myotubes (3).

We show here that RAGE activation and signaling in myoblasts result in reduced proliferation, migration, invasiveness, and matrix metalloproteinase (MMP) 1 and 2 activity, and increased apoptosis and adhesiveness, and that these effects rely on amphoterin/RAGE-dependent activation of p38 MAPK. We also show that inoculation into immunocompromised mice of myoblasts overexpressing a signaling-deficient RAGE mutant, but not mock-transfected myoblasts or myoblasts overexpressing full-length RAGE results in tumor formation.

EXPERIMENTAL PROCEDURES

Cell Culture Conditions, [³H]Thymidine Incorporation, Transfections, and Apoptosis and Luciferase Assays—Rat L6 myoblasts (clone L6C31) were cultured for 24 h in Dulbecco's modified Eagle's medium (DMEM) supplemented with 10% FBS (Invitrogen), 100 units/ml penicillin, and 100 μ g/ml streptomycin, in a H₂O-saturated 5% CO₂ atmosphere at 37 °C before decreasing FBS to 2% to induce myoblast differentiation. L6 myoblast clones stably overexpressing RAGE or RAGE Δ cyto were selected and characterized as described (15). Experiments were performed using mock-transfected, L6/RAGE and L6/RAGE Δ cyto myoblasts in 10 or 2% FBS as indicated in the legends to figures. The anti-amphoterin antibody (BD Pharmingen) used in some experiments was shown to neutralize culture medium amphoterin (16).

For [³H]thymidine incorporation assay, myoblasts (25 \times 10³ cells/well) were cultivated in 10% FBS for 24 h in 24-multiwell plates, washed with DMEM, serum-starved for 24 h, washed with DMEM, and cultivated in DMEM in the presence of either 10 or 2% FBS for another 24 h in the presence of 1 μ Ci of [³H]thymidine/ml. Parallel myoblasts treated in the same manner in the absence of [³H]thymidine were incubated with HOECHST 33258 (bisbenzimidazole) as described (25) to normalize incorporated [³H]thymidine to DNA content.

For cell number measurements, myoblasts were cultivated in 10% FBS for 24 h in 96-multiwell plates at a density of 4 \times 10³ cells/well and then in DMEM in the presence of either 10 or 2% FBS for 1–7 days. Cell

density was measured by a tetrazolium-based (MTT) colorimetric assay.

To analyze the cell cycle and measure apoptosis, myoblasts were seeded onto 35-mm plastic dishes (18 \times 10⁴ cells/dish) in 10% FBS for 24 h, washed with DMEM, and cultivated for 24 or 48 h in DMEM in the presence of either 10 or 2% FBS. Cells were stained with propidium iodide in hypotonic buffer and subjected to fluorescence-activated cell sorting (FACS) analysis as described (26). This procedure allows the determination of the percentage of apoptotic (hypodiploid) nuclei as well as that of normal (diploid) nuclei in the same cell population irrespective of the cell volume. In experiments performed in the presence of the p38 MAPK inhibitor, SB203580 (Calbiochem) (2 μ M, final concentration), control cells received an equal volume of vehicle (dimethyl sulfoxide). FACS analysis was also employed to measure the mean cell volume as described (27).

Transient transfections were carried out using Lipofectamine 2000 (Invitrogen) as recommended by the manufacturer. Briefly, myoblasts cultured in 10% FBS without antibiotics were transfected with the reporter gene p21^{Waf1}-*luc*, reporter gene cyclin D1-*luc*, or empty vector. After 6 h, cells were cultivated in 10 or 2% FBS, as indicated in the figure legends. After another 24 h cells were harvested to measure luciferase activity. p21^{Waf1} and cyclin D1 promoter transcriptional activities were normalized for transfection efficiency by cotransfecting cells with a cDNA encoding green fluorescent protein. The percentage of green fluorescent protein-positive cells (20 to 25%) was determined by FACS analysis.

Western Blot Analyses—To detect phosphorylated and total extracellular signal-regulated kinase (ERK) 1/2, phosphorylated and total c-Jun NH₂-terminal protein kinase (JNK), phosphorylated and total retinoblastoma suppressor protein Rb, tubulin, caspase-3, Bcl-2, integrin β 1, VCAM, NCAM, and caveolin-3 in myoblast extracts by Western blotting, myoblasts were cultivated as detailed in the legend of pertinent figures, washed twice with PBS, and solubilized with 2.5% SDS, 10 mM Tris-HCl, pH 7.4, 0.1 M dithiothreitol, 0.1 mM tosylsulfonylethyl chloromethyl ketone protease inhibitor (Roche). The following antibodies were used: polyclonal antibody specific to phosphorylated (Thr²⁰²/Tyr²⁰⁴) ERK1/2 (1:1,000, New England BioLabs), polyclonal anti-ERK1/2 antibody (1:5,000, Sigma), polyclonal anti-phosphorylated (Ser⁸⁰⁷/Ser⁸¹¹) Rb antibody (1:1,000, Cell Signaling Technology), polyclonal anti-Rb antibody (1:1,000, Cell Signaling Technology), monoclonal anti- α -tubulin antibody (1:10,000; Sigma), polyclonal anti-caspase-3 antibody (1:1,000; Cell Signaling Technology), polyclonal anti-Bcl-2 antibody (1:1,000; BD Pharmingen), monoclonal anti-integrin β 1 antibody (1:2,000; BD Transduction Laboratories), monoclonal anti-VCAM antibody (1:2,000; BD Pharmingen), monoclonal anti-NCAM antibody (1:2,000; Sigma), and monoclonal anti-caveolin-3 antibody (1:2,000; BD Transduction Laboratories). The immune reaction was developed by enhanced chemiluminescence (ECL) (SuperSignal West Pico, Pierce).

Adhesion, Migration, and Invasiveness Assays, and F-actin Staining—For adhesion experiments, mock-transfected, L6/RAGE, and L6/RAGE Δ cyto myoblasts (50 \times 10³ cells in 0.1 ml of DMEM containing 10% FBS) were seeded into each well, incubated for 3 h, and further processed as described (28, 29). The supernatant with non-adherent cells was removed by two washes with warmed culture medium. Attached cells were fixed with 30% methanol/ethanol for 15 min at room temperature, stained with 0.1% crystal violet (Sigma) in PBS, extensively washed with distilled water, and dried at room temperature. The dye was resuspended with 50 μ l of 0.2% Triton X-100/well, and color yield was measured using an enzyme-linked immunosorbent assay reader at 590 nm.

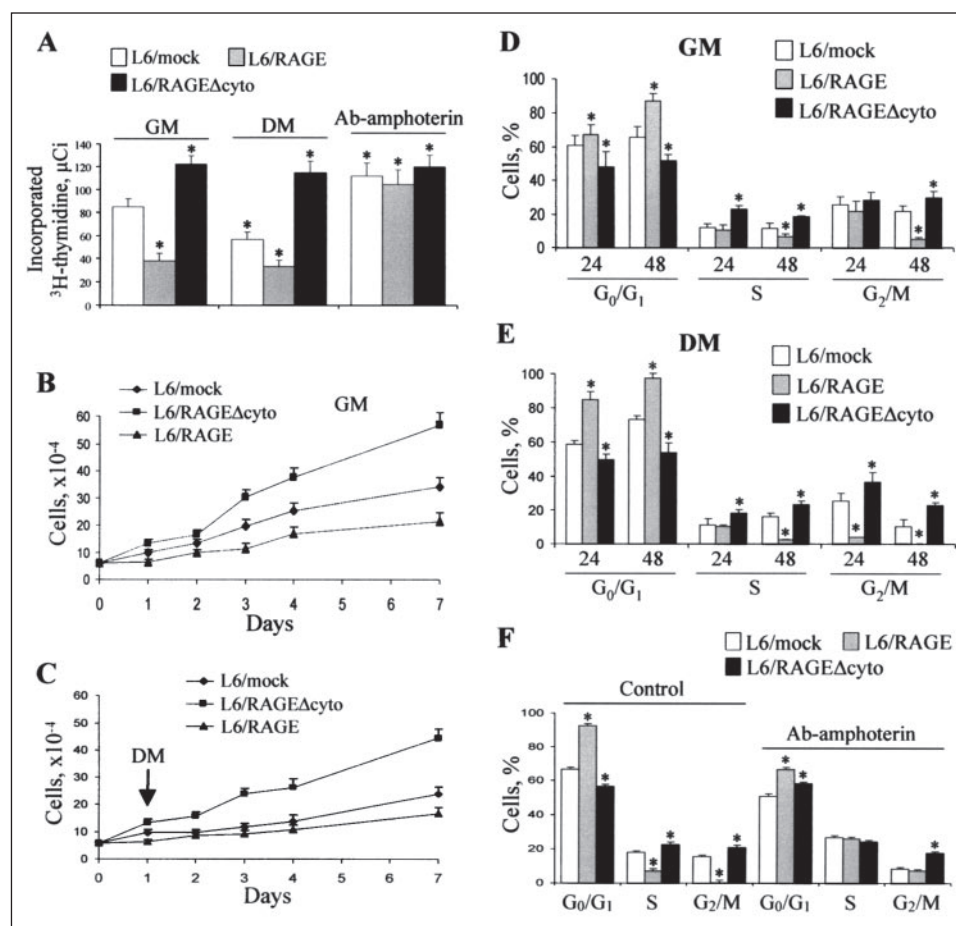


FIGURE 1. The amphoterin/RAGE pair negatively regulates myoblast proliferation. *A*, L6/mock, L6/RAGEΔcyto, and L6/RAGE myoblasts were cultivated for 24 h in GM (10% FBS) and serum-starved for another 24 h. Then, the medium was renewed in one series of cells (GM), whereas another series of cells was switched to differentiation medium (2% FBS) (DM). Parallel cells not serum-starved were given 2.5 μg/ml of an anti-amphoterin antibody at the time of the switch to DM. The control experiment performed with 2.5 μg/ml non-immune IgG (that gave similar results to the DM series without additions) is not shown. [³H]Thymidine (1 μCi) was added to myoblasts at the time of culture medium renewal or switch, and cells were cultivated for 24 h before processing for [³H]thymidine incorporation. *B* and *C*, same as in *A* except that after culture medium renewal (*B*) or switch to DM (*C*), myoblasts were cultivated for the times indicated and processed by MTT assay. *D* and *E*, same as in *A* except that after culture medium renewal (*D*) or switch to DM (*E*), myoblasts were cultivated for another 24 or 48 h as indicated and subjected to FACS analysis to measure the fractions of cells in the G₀/G₁, S, and G₂/M phases of the cell cycle. *F*, same as in *E* except that at the time of the culture medium switch to DM, myoblasts received either 2.5 μg/ml non-immune IgG or 2.5 μg/ml of an anti-amphoterin antibody for 48 h. Averages of three independent experiments ± S.D. Asterisk, significantly different from control ([³H]thymidine incorporation in L6/mock myoblasts in GM) (*p* < 0.05) (*A*); asterisk, significantly different from internal control (individual phases of the cell cycle in L6/mock myoblasts) (*p* < 0.05) (*D–F*).

For migration assay, we used Boyden chambers (pore size, 8 μm) (BD Biosciences). Individual myoblast clones (5 × 10⁴ cells in 0.5 ml of DMEM) were placed in the upper chamber, and 0.75 ml of DMEM containing 10% FBS was placed in the lower chamber. After 20 h in culture, cells on the upper side of the filters were removed with cotton-tipped swabs, and the filters were fixed in methanol for 2 min and stained with 0.05% crystal violet in PBS for 15 min. Cells on the underside of the filters were viewed and counted under a microscope. Each clone was plated in triplicate in each experiment. For the invasiveness assay, conditions were as described for migration assay except that bio-coat Matrigel invasion chambers (pore size, 8 μm) (BD Biosciences) were used.

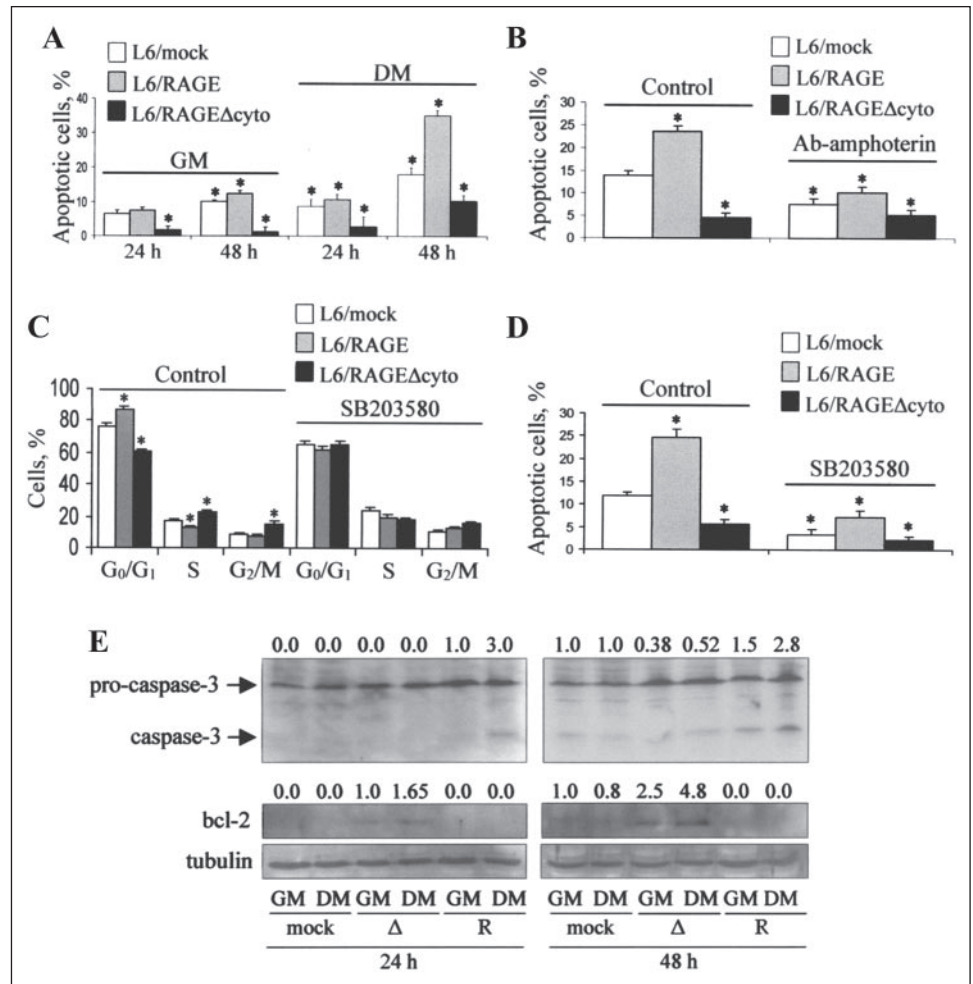
For F-actin staining, myoblasts were seeded onto 13-mm glass coverslips in plastic multiwell dishes (7.5 × 10⁴ cells/dish) in DMEM containing 10% FBS for 24 h and washed in PBS. Cells were then fixed for 10 min in 3.7% paraformaldehyde in PBS, extensively washed with PBS, permeabilized with 0.1% Triton X-100 in PBS for 2 min, washed again, and incubated with fluorescein-labeled phalloidin (Sigma) (1:250 in PBS) for 1 h in a humid chamber at room temperature. After three washes in PBS, the cells were mounted in 80% glycerol, containing 0.02% NaN₃ and *p*-phenylenediamine (1 mg/ml) in PBS to prevent fluores-

cence fading and viewed on a Leica DM Rb fluorescence microscope equipped with a digital camera.

Gelatin Zymography—Mock-transfected, L6/RAGE, and L6/RAGEΔcyto myoblasts were cultivated in a 150-cm² flask in DMEM containing 10% FBS, after which the supernatant was collected, centrifuged to remove detached cells, and concentrated. The protein concentration of the supernatants was determined using the Bio-Rad protein microassay system with bovine serum albumin as a standard. Samples were stored at -70 °C until use. Aliquots (10 μg of total protein per sample) were electrophoresed at constant voltage on a 10% polyacrylamide gel containing 2 mg/ml of gelatin. The gels were rinsed three times for 15 min in 2.5% Triton X-100 to remove SDS and renature the proteins and then incubated in MMP activation buffer (50 mM Tris-HCl, pH 7.5, with 5 mM CaCl₂) for 24 h at 37 °C with constant shaking. Gels were stained overnight in 0.5% Coomassie Blue R-250 and destained for 1 h in 40% methanol, 10% acetic acid. Proteinase activity was quantified by densitometric scanning.

In Vivo Tumor Growth—For tumor growth *in vivo*, female (NOD/SCID) mice weighing ~20 g were inoculated subcutaneously with 5 × 10⁶ L6/wt, L6/RAGEΔcyto, or L6/RAGE myoblasts and monitored for ~3.5 months. The mice were sacrificed by cervical dislocation. Consent was obtained by the Ethics Committee of the University of Perugia.

FIGURE 2. The amphoterin/RAGE pair stimulates apoptosis and inhibits proliferation via a p38 MAPK-dependent mechanism in L6 myoblasts. *A*, conditions were as described in the legend to Fig. 1, *D* and *E*, except that FACS analysis was employed to measure apoptosis in individual L6 clones. *B*, same as in *A* except that at the time of the culture medium switch to DM, myoblasts received either 2.5 $\mu\text{g/ml}$ non-immune IgG (control) or 2.5 $\mu\text{g/ml}$ of an anti-amphoterin antibody for 48 h. *C*, same as in *A* except that at the time of the switch to DM, myoblasts received 2 μM SB203580 (an inhibitor of p38 MAPK) in Me₂SO or an equal volume of Me₂SO (control) for 48 h before FACS analysis to measure the fractions of cells in the G₀/G₁, S, and G₂/M phases of the cell cycle. *D*, same as in *C* except that FACS analysis was employed to measure apoptosis in myoblasts in DM. *E*, myoblasts were cultivated 24 h in GM and then 24 h in DM, and subjected to Western blotting with either an anti-caspase-3 antibody to detect the fraction of activated caspase-3 or an anti-Bcl-2 antibody to detect Bcl-2 in individual L6 clones. Numbers on top of lanes refer to the fraction of activated caspase-3 relative to total caspase-3 or the fraction of Bcl-2 in L6/RAGE Δ cyto and L6/RAGE myoblasts relative to L6/mock myoblasts after normalization to tubulin as analyzed by densitometry. Mock, Δ , and R in *E* stand for L6/mock, L6/RAGE Δ cyto, and L6/RAGE myoblasts, respectively. Averages of three independent experiments \pm S.D. (*A–D*). One representative experiment of three (*E*). Asterisk in *A*, significantly different from control (percentage of apoptotic cells in L6/mock myoblasts after 24 h in GM, respectively), $p < 0.05$; asterisk in *B* and *D*, significantly different from control (percentage of apoptotic cells in L6/mock myoblasts after 48 h in DM), $p < 0.05$; asterisk, significantly different from internal control (*C*) (individual phases of the cell cycle in L6/mock myoblasts), $p < 0.05$.



Tumor masses were excised and weighed, and tumor volume was calculated by the equation: tumor volume = $x^2y/2$, where x and y correspond to the width and thickness of the tissue, respectively. Tumors were then fixed with 4% paraformaldehyde in PBS (2 days at 4 °C), extensively washed in PBS, and paraffin-embedded. Sections were stained with hematoxylin/eosin, and histopathology was performed by an independent pathologist.

Statistical Analysis—The data were subjected to analysis of variance with SNK post-hoc analysis using a statistical software package (GraphPad Prism version 4.00, GraphPad Software, San Diego, CA). Statistical significance was assumed when $p < 0.05$.

RESULTS

RAGE Activation in Myoblasts Reduces Proliferation and Stimulates Apoptosis: Role of Amphoterin and p38 MAPK—L6/RAGE Δ cyto myoblasts incorporated more [³H]thymidine and L6/RAGE myoblasts incorporated less [³H]thymidine than did L6/mock myoblasts in both GM and DM (Fig. 1A). By MTT assay, a larger number of L6/RAGE Δ cyto myoblasts and a smaller number of L6/RAGE myoblasts were obtained at any day of cultivation in both GM (Fig. 1B) and DM (Fig. 1C) between days 1 and 7, compared with L6/mock myoblasts. Moreover, after 1 and 2 days of cultivation in both GM (Fig. 1D) and DM (Fig. 1E) by FACS analysis a larger fraction of L6/RAGE Δ cyto myoblasts and a smaller fraction of L6/RAGE myoblasts were in the S and G₂/M phases of the cell cycle (with a low percentage of L6/RAGE myoblasts in G₂/M phase at 48 h, pointing to the inability of these cells to complete cell division),

and a smaller fraction of L6/RAGE Δ cyto myoblasts and a larger fraction of L6/RAGE myoblasts were in the G₀/G₁ phase, compared with L6/mock myoblasts. Collectively, these data suggested that RAGE might transduce an antiproliferative signal in myoblasts.

Neutralization of culture medium amphoterin with an anti-amphoterin antibody (16) resulted in an increased [³H]thymidine incorporation by L6/RAGE and L6/mock myoblasts compared with their respective controls, and no effects in the case of L6/RAGE Δ cyto myoblasts (Fig. 1A). Notably, on administration of anti-amphoterin antibody the levels of [³H]thymidine incorporation were similar in the three L6 clones under study. Neutralization of the culture medium amphoterin with an anti-amphoterin antibody also reduced the fractions of L6/mock and L6/RAGE myoblasts in the G₀/G₁ phase and increased those in S and G₂/M phases, whereas without an effect on L6/RAGE Δ cyto myoblasts (Fig. 1F). Thus, amphoterin appeared to exert a regulatory role on myoblast proliferation, promoting proliferation arrest via RAGE engagement and stimulation of RAGE transducing activity. This effect of amphoterin would add to the reported promyogenic activity of the protein via activation of a RAGE-Cdc42-Rac-MKK6-p38 MAPK pathway (16).

In addition to reduced proliferation, L6/RAGE myoblasts exhibited a larger extent of apoptosis than did L6/mock myoblasts which in turn showed a larger extent of apoptosis than did L6/RAGE Δ cyto myoblasts in both GM and DM, with larger percentages in DM than in GM as expected, after 1 day of cultivation (Fig. 2A). Similar results were obtained after 2 days of cultivation (Fig. 2A). Also, neutralization of

Rage Inhibits Myoblast Proliferation and Tumor Formation

culture medium amphoterin reduced apoptosis in both L6/mock and L6/RAGE myoblasts, whereas without effect in the case of L6/RAGE Δ cyto myoblasts (Fig. 2B), suggesting that amphoterin was the RAGE ligand involved in RAGE-dependent stimulation of myoblast apoptosis.

RAGE-dependent activation of p38 MAPK (16) was responsible for RAGE-mediated effects on myoblast proliferation and apoptosis. In fact, treatment with the p38 MAPK inhibitor, SB203580, reduced the fraction of L6/RAGE and L6/mock myoblasts in the S and G₂/M phases of the cell cycle and decreased the fraction of these cells in the G₀/G₁ phase, without affecting L6/RAGE Δ cyto myoblasts (Fig. 2C), and decreased apoptosis in L6/RAGE, L6/RAGE Δ cyto, and L6/mock myoblasts (Fig. 2D), probably because of lack of inhibition of Raf activity under these conditions (30).

RAGE-dependent regulation of myoblast apoptosis was further investigated by analyzing the levels of activated caspase-3 and the anti-apoptotic factor, Bcl-2. We found that L6/RAGE Δ cyto myoblasts in GM and DM exhibited a smaller extent and L6/RAGE myoblasts exhibited a larger extent of caspase-3 activation, compared with L6/mock myoblasts (Fig. 2E). Also, L6/RAGE Δ cyto myoblasts exhibited higher levels and L6/RAGE myoblasts exhibited lower levels of Bcl-2, compared with L6/mock myoblasts (Fig. 2E), suggesting that RAGE signaling might negatively regulate Bcl-2 expression in myoblasts. Collectively, these data suggested that, besides promoting myoblast differentiation (16), RAGE activation by amphoterin might cause proliferation arrest and promote apoptosis in myoblasts via stimulation of p38 MAPK.

RAGE Activation in Myoblasts Increases p21^{Waf1} Induction and Reduces Cyclin D1 Induction and Rb Phosphorylation—Because increased levels of the proliferation inhibitor p21^{Waf1} and decreased levels of cyclin D1 and extents of Rb phosphorylation accompany myoblast proliferation arrest and differentiation (24, 31–33), we next analyzed the role of the amphoterin/RAGE pair in p21^{Waf1} and cyclin D1 induction and extent of Rb phosphorylation. In both GM and DM, L6/RAGE Δ cyto myoblasts exhibited a smaller induction of p21^{Waf1}, a larger induction of cyclin D1, and higher levels of phosphorylated Rb, whereas the opposite was observed in L6/RAGE myoblasts, compared with L6/mock myoblasts (Fig. 3, A–C). Neutralization of culture medium amphoterin reduced the levels of p21^{Waf1} induction in L6/RAGE and L6/mock myoblasts to nearly those detected in L6/RAGE Δ cyto myoblasts (Fig. 3A). Similarly, neutralization of culture medium amphoterin resulted in an increase in cyclin D1 induction (Fig. 3B) and the extent of Rb phosphorylation (Fig. 3D) in L6/RAGE and L6/mock myoblasts to the levels observed in L6/RAGE Δ cyto myoblasts. These data suggested that induction of p21^{Waf1} and cyclin D1 and the extent of Rb phosphorylation in myoblasts is under the control of the amphoterin/RAGE pair signaling. Thus, we concluded that the amphoterin/RAGE pair might transduce antiproliferative signals in myoblasts via up-regulation of p21^{Waf1} induction, down-regulation of cyclin D1 induction, and reduction of Rb phosphorylation.

RAGE Activation in Myoblasts Results in ERK1/2 and JNK Inactivation—We have previously shown that the amphoterin/RAGE pair stimulates myogenic differentiation via a Rac1-Cdc42-MKK6-p38 MAPK pathway (16), and data in Figs. 1 and 2 suggest that amphoterin/RAGE-dependent inhibition of myoblast proliferation and stimulation of myoblast apoptosis also might rely on p38 MAPK activation. Because ERK1/2 and JNK are known to exert pro-mitogenic and/or pro-survival effects in myoblasts (15, 34), we next analyzed the extent of their phosphorylation (activation) in the three L6 myoblast clones under study. Higher levels of phosphorylated ERK1/2 (Fig. 4A) and JNK (Fig. 4B)

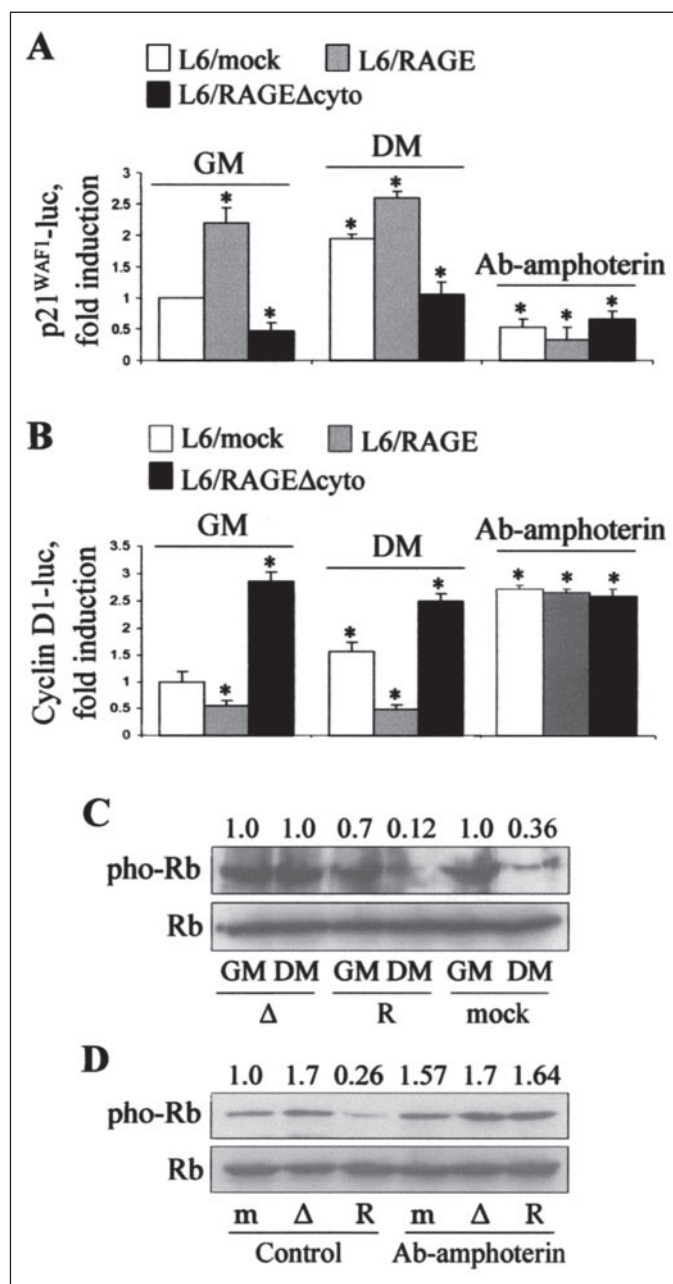


FIGURE 3. The amphoterin/RAGE pair stimulates p21^{Waf1} induction and reduces cyclin D1 induction and Rb phosphorylation in L6 myoblasts. A, L6/mock, L6/RAGE Δ cyto, and L6/RAGE myoblasts were cultivated for 24 h in GM (10% FBS) after which individual clones were transiently transfected with the p21^{Waf1}-luc reporter gene, further cultivated in GM or DM for 24 h as indicated, and processed to measure luciferase activity. Parallel cells were given 2.5 μ g/ml of an anti-amphoterin antibody at the time of the switch to DM. The control experiment performed with 2.5 μ g/ml non-immune IgG (that gave similar results to the DM series without additions) is not shown. B, same as in A except that individual L6 clones were transiently transfected with cyclin D1-luc reporter gene. C, L6/mock, L6/RAGE Δ cyto, and L6/RAGE myoblasts were cultivated for 24 h in GM (10% FBS) after which the culture medium was either renewed (GM) or switched to 2% FBS (DM). Cells were cultivated for another 24 h and subjected to Western blotting with anti-phosphorylated (phospho-Ser⁸⁰⁷/Ser⁸¹¹) Rb antibody or an anti-Rb antibody. D, same as in C except that at the time of the switch to DM, myoblasts received either 2.5 μ g/ml non-immune IgG (control) or of an anti-amphoterin antibody. Mock, Δ , and R in C and D stand for L6/mock, L6/RAGE Δ cyto, and L6/RAGE myoblasts, respectively. Numbers on top of lanes refer to the relative amount phosphorylated Rb (C and D). Averages of three independent experiments \pm S.D. are shown in A and B. One representative experiment of two is shown in C and D. Asterisk, significantly different from control (-fold induction in L6/mock myoblasts in GM), $p < 0.05$ (A and B).

were detected in L6/RAGE Δ cyto myoblasts in GM compared with L6/RAGE and L6/mock myoblasts, and low extents of ERK1/2 or JNK phosphorylation were observed in L6/RAGE myoblasts in DM (Fig. 4, A

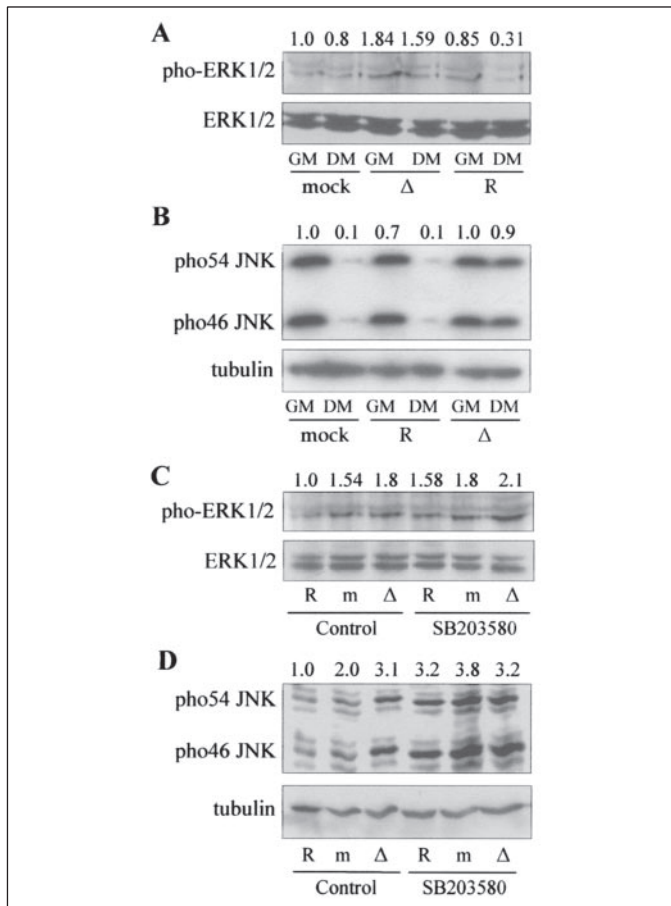


FIGURE 4. RAGE signaling reduces ERK1/2 and JNK phosphorylation in a p38 MAPK-dependent manner in L6 myoblasts. *A* and *B*, L6/mock, L6/RAGE Δ cyto, and L6/RAGE myoblasts were cultivated for 24 h in GM (10% FBS) and then in DM for 24 (*A*) or 48 h (*B*), washed and subjected to Western blotting with anti-phosphorylated ERK1/2 or anti-ERK1/2 (*A*), anti-phosphorylated JNK or anti-tubulin antibody (*B*). *C* and *D*, same as in *A* and *B* except that at the time of the switch to DM, myoblasts received 2 μ M SB203580 (an inhibitor of p38 MAPK) in Me₂SO or an equal volume of Me₂SO (control) for 24 h before Western blotting with anti-phosphorylated ERK1/2 or anti-ERK1/2 (*C*) and anti-phosphorylated JNK or anti-tubulin antibody (*D*). Mock, Δ , and R stand for L6/mock, L6/RAGE Δ cyto, and L6/RAGE myoblasts, respectively. Numbers on top of lanes refer to the relative amount of phosphorylated ERK1/2 or JNK (*A–D*). One representative experiment of two is shown in *A–D*.

and *B*). Moreover, levels of phosphorylated ERK1/2 and JNK were higher in L6/RAGE Δ cyto myoblasts compared with L6/mock myoblasts (Fig. 4, *A* and *B*), supporting the conclusion that RAGE signaling in L6 myoblasts might depress the activity of these kinases. Inhibition of p38 MAPK with SB203580 resulted in an increase in the extent of ERK1/2 (Fig. 4*C*) and JNK (Fig. 4*D*) phosphorylation in L6/RAGE and L6/mock myoblasts to the levels detected in L6/RAGE Δ cyto myoblasts. Thus, RAGE engagement caused inactivation of the mitogenic ERK1/2, likely via p38 MAPK-mediated inhibition of the Raf-MEK-ERK1/2 pathway (30), which might explain the antiproliferative and pro-apoptotic activity of RAGE as well as regulatory effects of RAGE signaling on induction of cyclin D1 and Rb phosphorylation, whereas the stimulatory effects of RAGE signaling on p21^{Waf1} induction could be ascribed to the activation of p38 MAPK (23). As to JNK, its inactivation by RAGE signaling might contribute to the observed decrease in proliferation of L6/RAGE and L6/mock myoblasts.

RAGE Activation in Myoblasts Increases Adhesiveness, Reduces Migration, Increases Cell Volume, and Up-regulates the Expression of Adhesion Molecules—Changes in adhesiveness and migration occur in myoblasts in coincidence with the initiation of terminal differentiation,

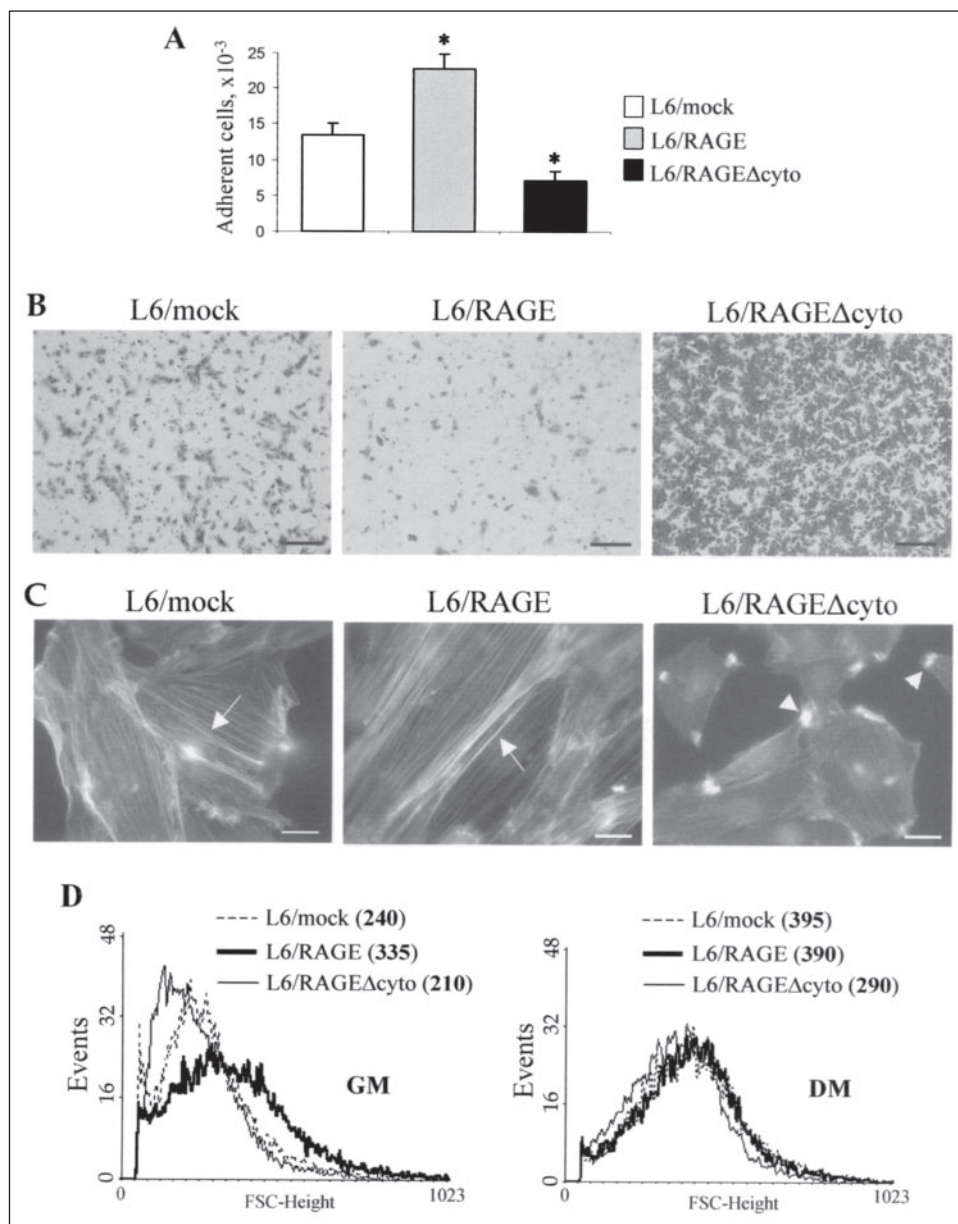
and these changes depend on expression of adhesion molecules shown to be important and/or crucial for myogenesis (35–43). Thus, we sought to analyze the three myoblast clones under study for adhesiveness, migration, invasiveness, and expression of adhesion molecules. L6/RAGE Δ cyto myoblasts exhibited decreased adhesiveness, increased migration and invasiveness, and decreased cell volume, whereas L6/RAGE myoblasts exhibited the opposite, compared with L6/mock myoblasts. Specifically, in a cell adhesiveness assay, 3 h after plating ~40% less L6/RAGE Δ cyto myoblasts and ~2 times more L6/RAGE myoblasts adhered to the substratum compared with L6/mock myoblasts (Fig. 5*A*). Qualitatively similar results were obtained at 24 h after plating (data not shown). Moreover, in a migration assay using Boyden chambers, a higher percentage of L6/RAGE Δ cyto myoblasts and a lower percentage of L6/RAGE myoblasts were recovered in the lower chamber, compared with L6/mock myoblasts (Fig. 5*B*), suggesting that RAGE signaling might influence myoblast motility. In addition, 1 day after culture in GM, L6/RAGE Δ cyto myoblasts exhibited a smaller size and L6/RAGE myoblasts exhibited a larger size, compared with L6/mock myoblasts, as investigated by F-actin decoration with fluorescein-labeled phalloidin (Fig. 5*C*) and FACS analysis (Fig. 5*D*). When analyses of cell size were performed on myoblasts in DM, a general increase in mean cell size was registered in individual L6 clones, compared with the respective counterpart in GM, but whereas L6/mock and L6/RAGE myoblasts exhibited a similar size, L6/RAGE Δ cyto myoblasts showed a significantly smaller size compared with the two other clones again pointing to different responses of L6/RAGE Δ cyto myoblasts from L6/mock and L6/RAGE myoblasts to the switch from GM to DM. Also, the F-actin cytoskeleton appeared well organized in L6/RAGE myoblasts and much less so in L6/RAGE Δ cyto myoblasts compared with L6/mock myoblasts (Fig. 5*C*). These data suggested that the transducing activity of RAGE in myoblasts might not be restricted to stimulation of differentiation (16), inhibition of proliferation, and stimulation of apoptosis (Fig. 1 and 2); RAGE activation also appeared to profoundly modify myoblast morphology and motility, suggesting that these changes might be mechanistically linked to RAGE-dependent stimulation of myoblast differentiation. In particular, functional inactivation of RAGE in L6 myoblasts resulted in a dramatic decrease in cell size along with a less organized F-actin cytoskeleton and increased filopodia formation (Fig. 5), as is typical of proliferating, migrating, and poorly adherent cells, the opposite being observed in myoblasts overexpressing RAGE.

As mentioned above, adhesion molecules (*e.g.* β_1 -integrin, NCAM, and VCAM) and caveolin-3 play an important role in myoblast adhesiveness and differentiation (35–43), and RAGE activation has been shown to result in an enhanced expression of VCAM, NCAM, and ICAM in other cell types (17, 18). We found that L6/RAGE Δ cyto myoblasts expressed lower levels, and L6/RAGE myoblasts expressed higher levels of β_1 -integrin, caveolin-3, NCAM, and VCAM, compared with L6/mock myoblasts, as investigated by both Western blotting (Fig. 6*A*) and immunofluorescence (Fig. 6*B*), suggesting that RAGE signaling contributed to up-regulate the expression of a set of adhesion molecules playing a fundamental role in myoblast fusion into myotubes. These data were in agreement with the observation that RAGE signaling in myoblasts resulted in enhanced adhesiveness (Fig. 5*A*) and, incidentally, they provide evidence for the first time that RAGE engagement can induce β_1 -integrin and caveolin-3 expression.

RAGE Signaling in Myoblasts Results in Increased Invasiveness and Reduced MMP-1 and MMP-2 Activity—Given the increased motility of L6/RAGE Δ cyto myoblasts and the decreased motility of L6/RAGE myoblasts reported above (Fig. 5*B*), we sought to determine whether RAGE might be implicated in the regulation of invasive properties of L6 myoblasts

Rage Inhibits Myoblast Proliferation and Tumor Formation

FIGURE 5. RAGE signaling increases adhesiveness and reduces motility in L6 myoblasts. *A*, L6/mock, L6/RAGE Δ cyto, and L6/RAGE myoblasts were seeded at a density of 3×10^4 cells/well into a 96-multiwell plate and cultivated for 3 h in GM (10% FBS) after which the medium was aspirated and attached cells were washed twice with culture medium, fixed in methanol/ethanol, and stained with crystal violet. Absorbance at 590 nm was used to calculate the number of adherent cells. *B*, same as in *A* except that myoblasts were seeded in Boyden chambers and processed to analyze cell migration as described under "Experimental Procedures." *C*, same as in *A* except that myoblasts cultivated in GM for 24 h were fixed and stained with fluorescein-labeled phalloidin. Arrows and arrowheads point to stress fibers and filopodia, respectively. *D*, same as in *C* except that after 24 h in GM, myoblasts were cultivated in DM for 24 or 48 h and processed for FACS analysis to measure the mean cell volume. Averages of three independent experiments \pm S.D. are shown in *A*. Asterisks, significantly different ($p < 0.05$) (*B–D*). One representative experiment of two is shown. Numbers in the legends in the GM and DM panels in *D* refer to the median distribution of cells. Bars = 250 μ m (*A*) and 20 μ m (*C*).



by an invasiveness assay and determination of MMP activity. In an invasiveness assay using Boyden chambers endowed with a Matrigel barrier, L6/RAGE Δ cyto myoblasts migrated to a larger extent through Matrigel, whereas L6/RAGE myoblasts behaved the opposite, compared with L6/mock myoblasts (Fig. 7A). Thus, functional inactivation of RAGE made L6 myoblasts more locally invasive, whereas RAGE activation reduced the invasive properties of L6 myoblasts. Alternatively, the increased volume of L6/RAGE myoblasts (Fig. 5, *C* and *D*) might have precluded migration through the 8- μ m pores of Boyden chambers.

MMP, *i.e.* proteases that are liberated into the extracellular space and are implicated in cell migration and invasiveness, have been shown to play a role in myogenesis (44). Specifically, activation of MMP-1 and MMP-2 have been proposed to be important for myoblasts migration and invasiveness both in early phases of skeletal muscle formation during embryogenesis, when proliferating myoblasts have to migrate to the places of muscle formation, and during muscle regeneration, when activated satellite cells have to migrate toward damaged myofibers. Also, the liberation and activity of these two MMPs are remarkably increased

in rhabdomyosarcomas (45), which are known to exhibit an exaggerated motility and invasiveness. On the other hand, MMP-9 seems to play a negligible role in myoblast migration and invasiveness normally, its liberation and activity likely being increased in the course of muscle regeneration (44). We analyzed the culture media of individual myoblast clones for MMP-1, MMP-2, and MMP-9 activity by zymography. An increased MMP-1 and MMP-2 activity and remarkably low MMP-9 activity were observed in L6/RAGE Δ cyto myoblast culture medium, compared with L6/mock myoblasts (Fig. 7B). By contrast, lower MMP-1 and MMP-2 activities were detected in the culture medium of L6/RAGE myoblasts, compared with L6/mock myoblasts (Fig. 7B). Thus, a close relationship was confirmed between myoblast migration and invasiveness and MMP-1 and -2 activity, and an inverse relationship was established between MMP-1 and -2 activity and the amount of RAGE expressed.

Collectively, these data suggested the possibility that RAGE might negatively regulate the release of certain MMPs in myoblasts and that repression of RAGE expression (here exemplified by functional inactivation of RAGE) might confer increased motility and invasiveness upon

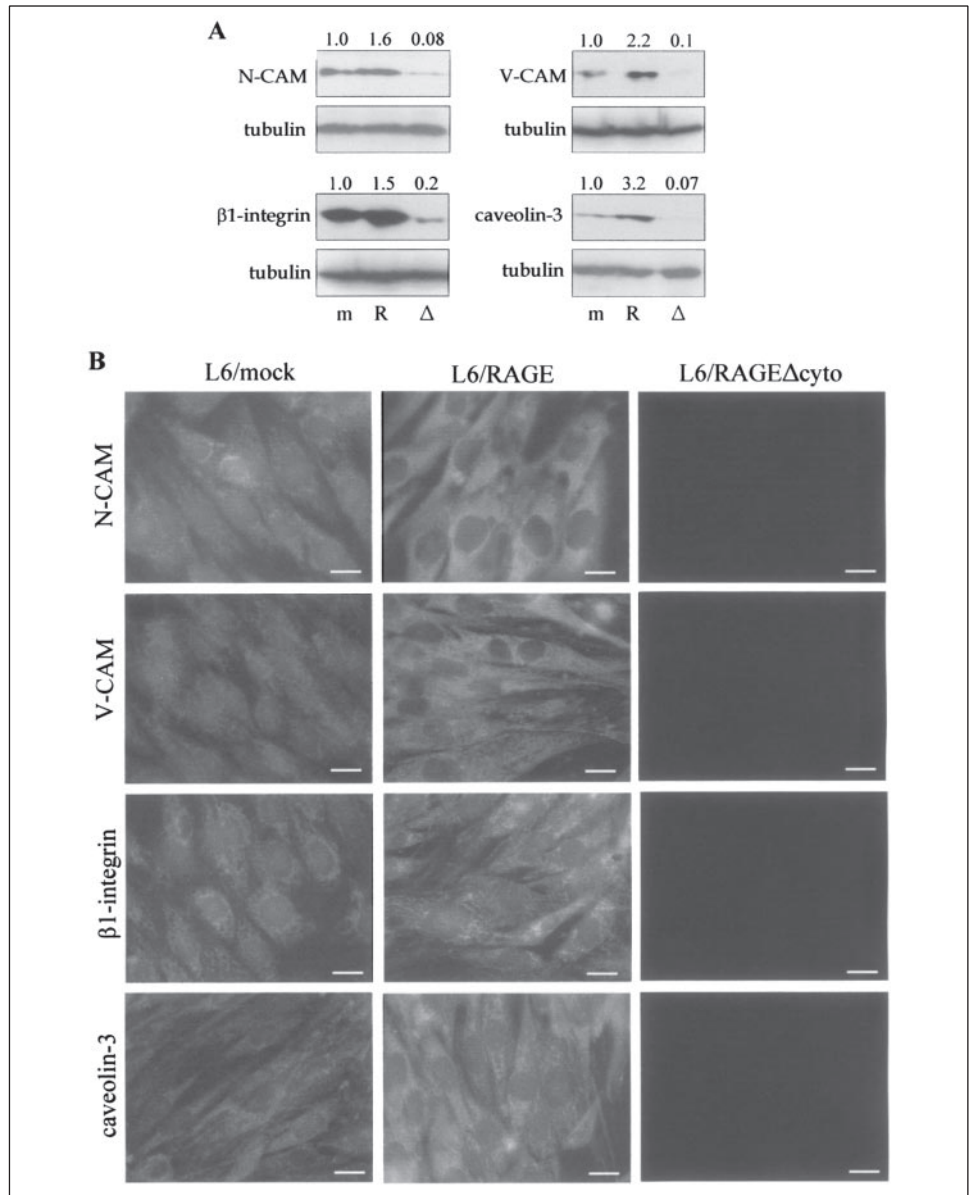


FIGURE 6. RAGE signaling stimulates integrin β 1, VCAM, NCAM, and caveolin-3 expression in L6 myoblasts. *A*, L6/mock, L6/RAGE Δ cyto, and L6/RAGE myoblasts were cultivated for 24 h in GM (10% FBS), switched to DM (2% FBS), and left undisturbed for 6 days under these conditions, washed and subjected to Western blotting with an anti-integrin β 1, anti-VCAM, anti-NCAM, or anti-caveolin-3 antibody. A Western blot of tubulin is included to show loading of equal amounts of proteins in individual lanes. Numbers on top of lanes refer to relative amounts of individual adhesion proteins in the three L6 clones after normalization to tubulin. One representative experiment of two is shown. *Mock*, Δ and *R*, in *E* stand for L6/mock, L6/RAGE Δ cyto, and L6/RAGE myoblasts, respectively. *B*, same as in *A* except that myoblasts were cultivated for 3 days in DM, fixed, and subjected to immunofluorescence with an anti-integrin β 1, anti-VCAM, anti-NCAM, or anti-caveolin-3 antibody as indicated. One representative experiment of two is shown. Bars = 20 μ m (*B*).

myoblasts that was also manifested by an increased MMP-1 and -2 activity. As to MMP-9, its low extent of activity in L6/RAGE myoblasts might be in accordance with it not playing a major role in myoblast migration and invasiveness (44).

Inoculation of L6/RAGE Δ cyto Myoblasts Results in Tumor Formation *in Vivo*—Next we inoculated immunocompromised mice with L6/RAGE, L6/RAGE Δ cyto, or L6/mock myoblasts, and tumor formation was monitored for \sim 3.5 months. All five mice injected with L6/RAGE Δ cyto myoblasts, three of five mice injected with L6/RAGE myoblasts, and two of five mice injected with L6/mock myoblasts developed a tumor mass (Fig. 8A). However, tumor formation in the case of L6/RAGE Δ cyto myoblasts preceded that of L6/RAGE and L6/mock myoblasts by \sim 4 weeks, and mean volume and weight of tumor masses were \sim 2.5 times larger in the case of L6/RAGE Δ cyto myoblasts compared with L6/RAGE and L6/mock myoblasts (Fig. 8B). Moreover, large areas of necrosis in the central core of the tumor and neovascularization at the tumor periphery were detected in L6/RAGE Δ cyto myoblast tumors, whereas L6/RAGE and L6/mock masses were essentially devoid of necrosis (Fig. 8C), and the tumor tissue invaded the neighboring skeletal

muscle tissue in the case of L6/RAGE Δ cyto myoblasts only (data not shown). Lastly, L6/RAGE Δ cyto myoblasts in the tumor mass appeared mostly as densely packed, round cells, whereas L6/RAGE and L6/mock myoblasts appeared elongated and hypertrophic, *i.e.* similar to myoblasts ready for fusion (Fig. 8C). Indeed, elongated and hypertrophic myoblasts could be detected in L6/mock myoblasts and even more so in L6/RAGE myoblasts (Fig. 8C, arrows). Thus, masses formed in mice inoculated with L6/RAGE Δ cyto myoblasts exhibited characteristics of authentic tumors, whereas those formed in mice inoculated with L6/RAGE and L6/mock myoblasts did not, and the higher incidence of tumor mass formation in mice inoculated with L6/RAGE myoblasts compared with those inoculated with L6/mock myoblasts likely depended on the larger volume of L6/RAGE and L6/mock myoblasts rather than on uncontrolled proliferation. In conclusion, overexpression of signaling-deficient RAGE conferred an aggressive potential on L6 myoblasts.

DISCUSSION

RAGE, a multiligand receptor of the immunoglobulin superfamily, has been implicated in the inflammatory response, neuronal trophism,

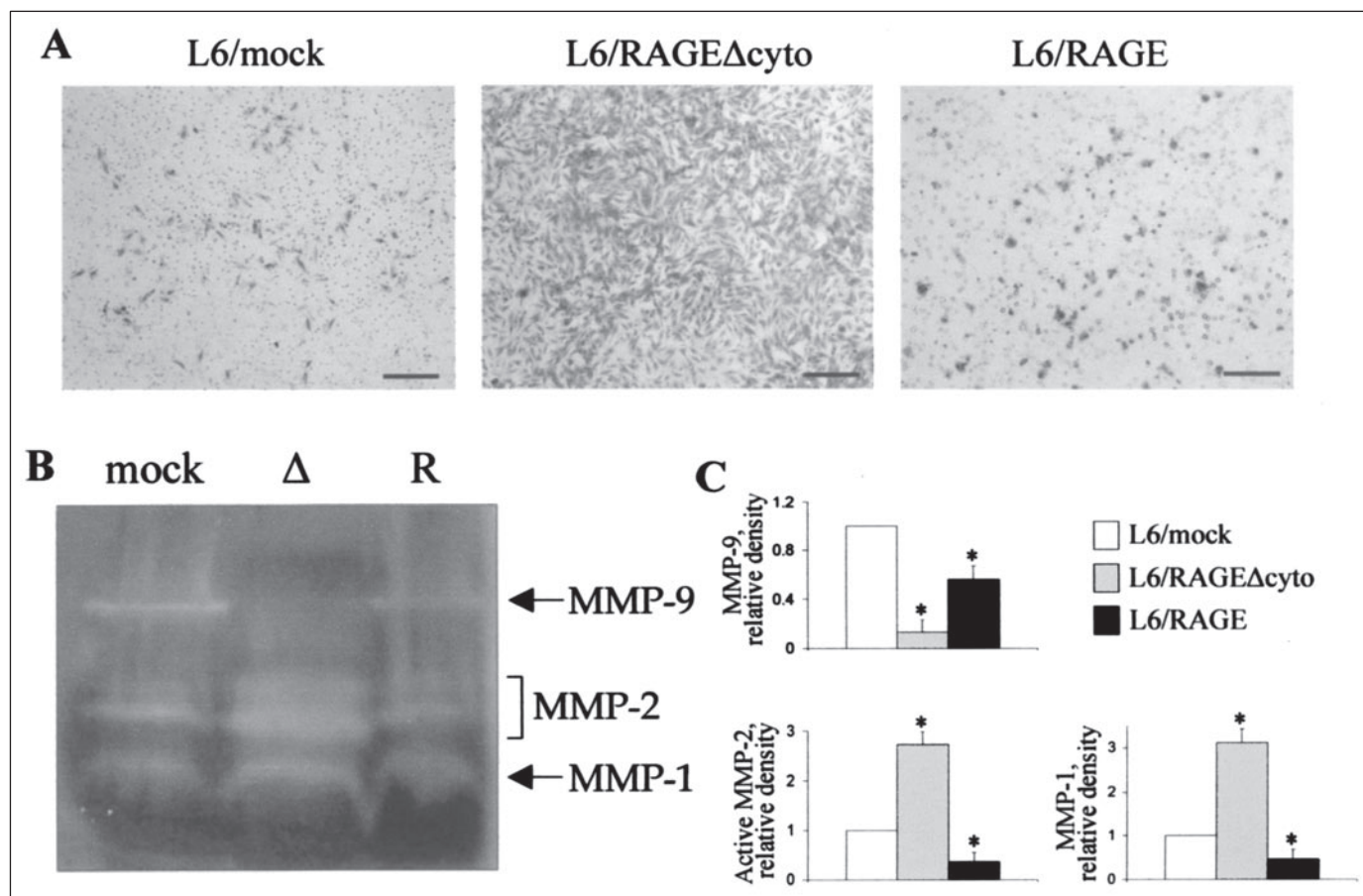


FIGURE 7. RAGE signaling in L6 myoblasts reduces invasiveness and modulates MMP release. A, L6/mock, L6/RAGEΔcyto, and L6/RAGE myoblasts were seeded at a density of 3×10^4 cells/well into Boyden chambers endowed with a Matrigel barrier. Next, steps were as described under "Experimental Procedures" to analyze invasiveness. One representative experiment of three is shown. B, L6/mock, L6/RAGEΔcyto, and L6/RAGE myoblasts were cultivated for 24 h in GM (10% FBS) after which the culture medium was subjected to zymography to detect the relative MMP-1, MMP-2, and MMP-9 activities. One representative experiment of three is shown. C, densitometric analysis of MMP-1, MMP-2, and MMP-9 activities in the culture medium of L6/mock, L6/RAGEΔcyto, and L6/RAGE myoblasts. Mock, Δ, and R in B stand for L6/mock, L6/RAGEΔcyto, and L6/RAGE myoblasts, respectively. Averages of three independent experiments \pm S.D. is shown. Asterisk, significantly different from control (MPP activity in the culture medium of L6/mock myoblasts), $p < 0.05$. Bars = 250 μ m (A).

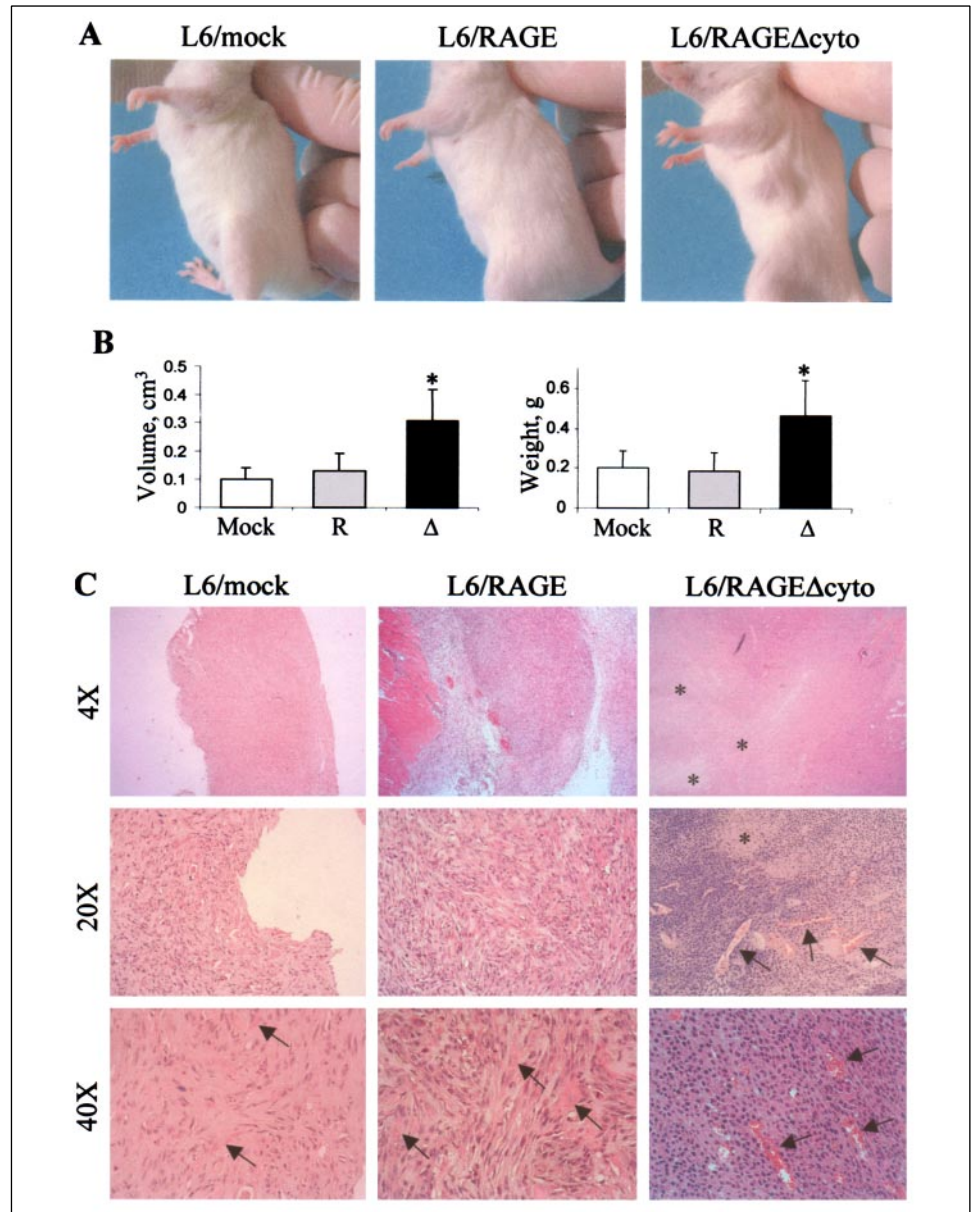
and neuronal death (depending on the nature of the ligand and the intensity and duration of the stimulus), and tumorigenesis (17). One prominent feature of RAGE is that it is expressed during development, repressed at completion of development, and re-expressed under certain pathological conditions (17). We reported that RAGE is expressed in rat skeletal myofibers during fetal development and up to ~11 days after birth, disappearing thereafter (16), suggesting that it might play a regulatory role in skeletal muscle formation. We also found that RAGE is expressed by rat L6 myoblasts and transduces a promyogenic signal via a Cdc42-Rac-MKK6-p38 MAPK pathway upon activation by its ligand, amphoterin (16). Similar results were obtained using the mouse C2C12 myoblast cell line.⁴ In the present work we show that, additionally, RAGE engagement by amphoterin contributes to myoblast proliferation arrest and apoptosis, two events strictly connected with the activation of the myogenic program (1, 3, 4, 46), and that this activity relies on p38 MAPK activation. We also show that RAGE engagement contributes to the increased adhesiveness and reduced motility of differentiating myoblasts, and, conversely, that reduction of RAGE transducing activity results in a decreased adhesiveness and increased motility and invasiveness of myoblasts. Finally, mice inoculated with L6/RAGEΔcyto myoblasts grow much larger, more aggressive, and more precocious tumor masses and with a higher incidence compared

with L6/RAGE or L6/mock myoblasts, and signs of authentic tumor formation can be observed in masses formed upon inoculation with L6/RAGEΔcyto myoblasts only.

Several lines of evidence support these conclusions. First, L6/RAGEΔcyto myoblasts proliferate more and L6/RAGE myoblasts proliferate less than L6/mock myoblasts, as investigated by [³H]thymidine incorporation, MTT assays, and FACS analysis, with consistent changes in the extent of activation of the pro-mitogenic kinases, ERK1/2 and JNK, of induction of the myoblast proliferation inhibitor, p21^{Waf1}, and cyclin D1, and of levels of phosphorylated Rb (Figs. 1 and 4). Second, lower and higher extents of apoptosis and caspase-3 activation were measured in L6/RAGEΔcyto and L6/RAGE myoblasts, respectively, and higher and lower levels of the anti-apoptotic factor, Bcl-2, were detected in L6/RAGEΔcyto and L6/RAGE myoblasts, respectively, compared with L6/mock myoblasts (Fig. 2). Third, inhibition of p38 MAPK results in a reduction of RAGE-dependent effects on myoblast proliferation and apoptosis (Fig. 2). Fourth, neutralization of culture medium amphoterin negates the effects of RAGE signaling in L6/mock and L6/RAGE myoblasts with no effects in L6/RAGEΔcyto myoblasts (Figs. 1–3). Last, a direct relationship is observed between expression of signaling-competent RAGE in myoblasts and myoblast size and adhesiveness, and, conversely, an inverse relationship is observed with respect to migration and invasiveness, L6/RAGEΔcyto myoblasts exhibiting reduced adhesiveness and enhanced migration and invasiveness compared with

⁴ F. Riuzzi, G. Sorci, and R. Donato, unpublished results.

FIGURE 8. Functional inactivation of RAGE in L6 myoblasts results in tumor formation. Immuno-compromised (NOD/SCID) mice were injected with L6/RAGE, L6/RAGE Δ cyto, or L6/mock myoblasts and tumor mass formation was followed for 3.5 months. After excision, tumor masses were analyzed for volume and weight (A and B) and histopathology (C). Before fixation, samples of individual tumor masses were subjected to RT-PCR to confirm expression of endogenous RAGE in tumors arising from injected L6/mock myoblasts and expression of human RAGE Δ cyto and human RAGE in tumors arising from injected L6/RAGE Δ cyto myoblasts and L6/RAGE myoblasts, respectively (data not shown). Tumor incidence was 100, 80, and 40% in the cases of L6/RAGE Δ cyto, L6/RAGE, and L6/mock myoblasts, respectively, and tumor volume and weight were ~2.5 times greater in L6/RAGE Δ cyto (Δ) tumors than L6/RAGE (R) and L6/mock (mock) tumors (A and B). However, ample zones of necrosis were detected in L6/RAGE Δ cyto tumors (asterisks) that were absent in L6/mock and L6/RAGE tumors, and neovascularization was detected at the periphery of the L6/RAGE Δ cyto tumor tissue (arrows in C, 20 and 40 \times L6/RAGE Δ cyto panels). Also, elongated and hypertrophic cells could be observed in masses formed upon inoculation with L6/mock myoblasts and even more so for L6/RAGE myoblasts (arrows in C, L6/mock and L6/RAGE panels, 40 \times) as opposed to the round cells found in L6/RAGE Δ cyto tumor masses (C, 40 \times). Asterisk, significantly different from control (first column from left in the average volume and weight panel in B) ($n = 5, p < 0.05$).



L6/mock and L6/RAGE myoblasts (Figs. 5 and 7). Consistent with this conclusion, we found that RAGE engagement and signaling positively regulate the expression of adhesion molecules shown to be important for myogenesis and negatively regulate MMP-1 and -2 liberation and activity (Figs. 6 and 7). Last, masses with the histological features of tumors form upon inoculation of immunocompromised mice with L6/RAGE Δ cyto, but not L6/mock or L6/RAGE myoblasts (Fig. 8). Most of the experiments described in the present report were performed using three independent L6 stable clones expressing similar amounts of RAGE or RAGE Δ cyto, with similar results (data not shown).

Functional inactivation of RAGE signaling results in higher levels of ERK1/2 and JNK phosphorylation compared with L6 mock-transfected myoblasts (Fig. 4), suggesting that signaling competent RAGE might inactivate these mitogenic kinases. Accordingly, levels of ERK1/2 and JNK phosphorylation are very low in myoblasts overexpressing RAGE (Fig. 4). This effect of RAGE signaling depends on activation of p38 MAPK because inhibition of p38 MAPK by use of SB203580 results in higher levels of ERK1/2 and JNK phosphorylation in L6/RAGE Δ cyto,

L6/mock, and L6/RAGE myoblasts, compared with their respective controls, with similar extents of phosphorylation in the three L6 clones under study (Fig. 4). These findings suggest that RAGE signaling to p38 MAPK might cause inactivation of ERK1/2, likely via inhibition of Raf activity (30), as well as of JNK. Moreover, higher levels of phosphorylated Rb and cyclin D1 and lower levels of the proliferation inhibitor, p21^{Waf1}, are detected in L6/RAGE Δ cyto myoblasts, whereas the opposite occurs in L6/RAGE myoblasts, compared with L6/mock myoblasts (Fig. 3). Because proliferation arrest, consequent to ERK1/2 and/or JNK inactivation, is a critical step in the context of myoblast terminal differentiation (at least at early phases of myogenic differentiation) (3, 15, 23, 34), RAGE-dependent inhibition of myoblast proliferation might thus be functional to the subsequent myoblast differentiation operated via p38 MAPK activation. We have previously reported that inhibition of p38 MAPK eliminates the ability of the amphotericin/RAGE pair to stimulate myogenesis (16).

It is known that under differentiation conditions a subpopulation of myoblasts undergoes differentiation and fusion into myotubes, another subpopulation remains undifferentiated and becomes quiescent, and

Rage Inhibits Myoblast Proliferation and Tumor Formation

still another subpopulation undergoes apoptosis (47–51). This latter event might serve to reduce the population of non-fused myoblasts coexisting with myotubes thus keeping the population of quiescent myoblast relatively low. We found that functional inactivation of RAGE signaling results in lower levels of myoblast apoptosis under both proliferation and differentiation conditions via reduction of levels of activated caspase-3 and up-regulation of Bcl-2 expression, compared with mock-transfected myoblasts, whereas the opposite occurs in myoblasts overexpressing RAGE (Fig. 2). Thus, RAGE signaling might contribute to the apoptosis usually taking place during the myoblast differentiation process. The ability of RAGE signaling to inactivate ERK1/2 might be responsible for this effect because inactivation of ERK1/2 by other means (e.g. by use of the ERK1/2 inhibitor, PD98059) also results in increased myoblast apoptosis (52–55).

Amphoterin/RAGE-dependent inactivation of ERK1/2 in myoblasts and the consequent down-regulation of Bcl-2 are at variance with respect to neurons in which RAGE engagement by amphoterin or low doses of S100B, another RAGE ligand, results in protection against apoptosis via stimulation of ERK1/2 and up-regulation of Bcl-2 expression (56). These data, whereas supporting the notion that RAGE can activate various signaling pathways (17), suggest that RAGE engagement might preferentially activate one particular signaling pathway over other ones in the different cell types in which the receptor operates thereby regulating specific functions. In myoblasts, the amphoterin/RAGE pair appears to mainly activate p38 MAPK via Cdc42-Rac1-MKK6 (16) with consequent depression of ERK1/2 and JNK activities (Fig. 4) and stimulation of myogenic differentiation (16), inhibition of proliferation, and enhancement of apoptosis (Figs. 1 and 2). These observations suggest that different intermediates acting immediately downstream of RAGE might operate in different cell types to specify the RAGE signaling activity. Additionally (or alternatively), different cell types might express distinct RAGE variants (57) that might account for cell specificity of RAGE effects. Whereas in principle the combination of the inhibitory effect of RAGE signaling on myoblast proliferation and its stimulatory effect on apoptosis might be detrimental during myogenesis and muscle regeneration, leading to a decreased myoblast density, its stimulatory effect on the promyogenic p38 MAPK might instead provide a means for accelerating myoblast terminal differentiation and fusion. Actually, in cultures of 80–90% confluent myoblasts, the overall effect of RAGE signaling is stimulation of myotube formation, which is best evident after the switch from proliferation conditions to differentiation conditions, but also detectable under proliferation conditions (16).

RAGE engagement in myoblasts also result in an increased adhesiveness and a decreased migration and invasiveness (Figs. 5 and 7). Myoblast proliferation arrest and the initiation of terminal differentiation are accompanied by an increased adhesiveness and expression of adhesion molecules and a decreased motility (3). Inhibition of RAGE signaling by overexpression of RAGE Δ cyto results in decreased adhesiveness and reduced expression of adhesion molecules (i.e. integrin β 1, VCAM, and NCAM) and caveolin-3, and an increased migration and invasiveness, whereas the opposite occurs in myoblasts overexpressing signaling-competent RAGE (Figs. 5–7). Because each one of the molecules listed above plays a fundamental role in myoblast fusion into myotubes (35–43), we conclude that RAGE signaling might reduce myoblast migration and accelerate fusion by contributing to the expression of those adhesion molecules in myoblasts.

Finally, we observe that L6/RAGE Δ cyto myoblasts liberate larger amounts of MMP-1 and -2 as inferred by zymography, the opposite occurring in L6/RAGE myoblasts, compared with L6/mock myoblasts (Fig. 7), in accordance with the increased migration and invasiveness of

L6/RAGE Δ cyto myoblasts and decreased migration and invasiveness of L6/RAGE myoblasts as well as changes in the expression of adhesion molecules mentioned earlier. These findings suggest that RAGE-dependent reduction of MMP-1 and -2 activity might contribute to decrease and/or interrupt myoblast migration thereby contributing to myoblast alignment for subsequent fusion into myotubes and, conversely, repression of RAGE expression might be functional to myoblast migration and/or contribute to the increased motility and invasiveness of, e.g. myoblast neoplastic counterparts. In fact, inoculation of L6/RAGE Δ cyto myoblasts into scid mice results in much larger and more aggressive tumor formation, compared with L6/RAGE or L6/mock myoblasts. Also, work in progress suggests that rhabdomyosarcoma cell lines that do not express RAGE undergo proliferation arrest and terminal differentiation, exhibit reduced migration and invasiveness, and grow much smaller tumor masses *in vivo* upon transfection with signaling-competent RAGE, compared with signaling-incompetent RAGE.⁵

In conclusion, our data provide evidence that, besides stimulating myoblast differentiation, RAGE engagement by amphoterin contributes to proliferation arrest of differentiating myoblasts, and that all of these effects rely on p38 MAPK activation. We also show that RAGE signaling results in the up-regulation of expression of adhesion molecules (i.e. integrin β 1, VCAM, and NCAM) and caveolin-3 that have been shown to play crucial roles in myoblast fusion into myotubes. We speculate that RAGE might be active at precise phases of embryonic myogenesis, i.e. in coincidence with myoblast proliferation arrest, initiation of terminal differentiation, and fusion into myotubes, thereby taking part in these events, and that repression of RAGE expression and/or signaling in myoblasts might contribute to the increased migration and invasiveness occurring in myoblast migration during embryonic myogenesis and/or muscle regeneration, and the increased migration invasiveness and *in vivo* aggressiveness typical of myoblast neoplastic counterparts.

Acknowledgment—We thank Eyal Bengal (Haifa, Israel) for providing the p21^{Waf1}-luc and cyclin D1-luc constructs.

REFERENCES

1. Andres, V., and Walsh, K. (1996) *J. Cell Biol.* **132**, 657–666
2. Arnold, H. H., and Winter, B. (1998) *Curr. Opin. Genet. Dev.* **8**, 539–544
3. Charge, S. B., and Rudnicki, M. A. (2004) *Physiol. Rev.* **84**, 209–238
4. Bennett, A. M., and Tonks, N. K. (1997) *Science* **278**, 1288–1291
5. Massague, J., Cheifetz, S., Endo, T., and Nadal-Ginard, B. (1986) *Proc. Natl. Acad. Sci. U. S. A.* **83**, 8206–8210
6. Florini, J. R., Ewton, D. Z., and Coolican, S. A. (1996) *Endocr. Rev.* **17**, 481–517
7. Maina, F., Casagrande, F., Audero, E., Simeone, A., Comoglio, P. M., Klein, R., and Ponzetto, C. (1996) *Cell* **87**, 531–542
8. Coolican, S. A., Samuel, D. S., Ewton, D. Z., McWade, F. J., and Florini, J. R. (1997) *J. Biol. Chem.* **272**, 6653–6662
9. Bour, B. A., Chakravarti, M., West, J. M., and Abmayr, S. M. (2000) *Genes Dev.* **14**, 1498–1511
10. Ruiz-Gomez, M., Coutts, N., Price, A., Taylor, M. V., and Bate, M. (2000) *Cell* **102**, 189–198
11. Langen, R. C., Schols, A. M., Kelders, M. C., Wouters, E. F., and Janssen-Heininger, Y. M. (2001) *FASEB J.* **15**, 1169–1180
12. Tortorella, L. L., Milasincic, D. J., and Pilch, P. F. (2001) *J. Biol. Chem.* **276**, 13709–13717
13. McCroskery, S., Thomas, M., Maxwell, L., Sharma, M., and Kambadur, R. (2003) *J. Cell Biol.* **162**, 1135–1347
14. Kang, J. S., Yi, M. J., Zhang, W., Feinleib, J. L., Cole, F., and Krauss, R. S. (2004) *J. Cell Biol.* **167**, 493–504
15. Sorci, G., Agneletti, A. L., Riuzzi, F., Marchetti, C., and Donato, R. (2003) *Mol. Cell Biol.* **23**, 4870–504
16. Sorci, G., Riuzzi, F., Arcuri, C., Giambanco, I., and Donato, R. (2004) *Mol. Cell Biol.*

⁵ F. Riuzzi, G. Sorci, and R. Donato, manuscript in preparation.

- 24, 4880–4894
17. Schmidt, A. M., Yan, S. D., Yan, S. F., and Stern, D. M. (2001) *J. Clin. Investig.* **108**, 949–955
 18. Muller, S., Scaffidi, P., Degryse, B., Bonaldi, T., Ronfani, L., Agresti, A., Beltrame, M., and Bianchi, M. E. (2001) *EMBO J.* **20**, 4337–4340
 19. Huttunen, H. J., and Rauvala, H. (2004) *J. Intern. Med.* **255**, 351–366
 20. Palumbo, R., Sampaolesi, M., De Marchis, F., Tonlorenzi, R., Colombetti, S., Mondino, A., Cossu, G., and Bianchi, M. E. (2004) *J. Cell Biol.* **164**, 441–449
 21. Cuenda, A., and Cohen, P. (1999) *J. Biol. Chem.* **274**, 4341–4346
 22. Li, Y., Jiang, B., Ensign, W. Y., Vogt, P. K., and Han, J. (2000) *Cell. Signal.* **12**, 751–757
 23. Wu, Z., Woodring, P. J., Bhakta, K. S., Tamura, K., Wen, F., Feramisco, J. R., Karin, M., Wang, J. Y. J., and Puri, P. L. (2000) *Mol. Cell. Biol.* **20**, 3951–3964
 24. Zetser, A., Gredinger, E., and Bengal, E. (1999) *J. Biol. Chem.* **274**, 5193–5200
 25. Rao, J., and Otto, W. R. (1992) *Anal. Biochem.* **207**, 186–192
 26. Nicoletti, L., Migliorati, G., Pagliacci, M. C., Grignani, F., and Riccardi, C. (1991) *J. Immunol. Methods* **139**, 271–279
 27. Ahmadzadeh, M., Hussain, S. F., and Faber, D. L. (1999) *J. Immunol.* **163**, 3053–3063
 28. Tietze, L., Borntraeger, J., Klosterhalfen, B., Amo-Takyi, B., Handt, S., Gunther, K., and Merkelbach-Bruse, S. (1999) *Exp. Mol. Pathol.* **66**, 131–139
 29. Aumailley, M., Mann, K., von der Mark, H., and Timpl, R. (1989) *Exp. Cell Res.* **181**, 463–474
 30. Lee, J., Hong, F., Kwon, S., Kim, S. S., Kim, D. O., Kang, H. S., Lee, S. J., Ha, J., and Kim, S. S. (2002) *Biochem. Biophys. Res. Commun.* **298**, 765–771
 31. Missero, C., Calautti, E., Eckner, R., Chin, J., Tsai, L. H., Livingston, D. M., and Dotto, G. P. (1995) *Proc. Natl. Acad. Sci. U. S. A.* **92**, 5451–5455
 32. Rao, S. S., and Kohtz, D. S. (1995) *J. Biol. Chem.* **270**, 4093–4100
 33. Porrello, A., Cerone, M. A., Coen, S., Gurtner, A., Fontemaggi, G., Cimino, L., Piaggio, G., Sacchi, A., and Soddu, S. (2000) *J. Cell Biol.* **151**, 1295–1304
 34. Puri, P. L., and Sartorelli, V. (2000) *J. Cell. Physiol.* **185**, 155–173
 35. Fazeli, S., Wells, D. J., Hobbs, C., and Walsh, F. S. (1996) *J. Cell Biol.* **135**, 241–251
 36. Hodges, B. L., Hayashi, Y. K., Nonaka, I., Wang, W., Arahata, K., and Kaufman, S. J. (1997) *J. Cell Sci.* **110**, 2873–2881
 37. Minetti, C., Sotgia, F., Bruno, C., Scartezzini, P., Broda, P., Bado, M., Masetti, E., Mazzocco, M., Egeo, A., Donati, M. A., Volonté, D., Galbiati, F., Cordone, G., Briccarelli, F. D., Lisanti, M. P., and Zara, F. (1998) *Nat. Genet.* **18**, 365–368
 38. Galbiati, F., Volonté, D., Engelman, J. A., Scherer, P. E., and Lisanti, M. P. (1999) *J. Biol. Chem.* **274**, 30315–30321
 39. Biederer, C. H., Ries, S. J., Moser, M., Florio, M., Israel, M. A., McCormick, F., and Buettner, R. (2000) *J. Biol. Chem.* **275**, 26245–26251
 40. Burkin, D. J., Wallace, G. Q., Nicol, K. J., Kaufman, D. J., and Kaufman, S. J. (2001) *J. Cell Biol.* **152**, 1207–1218
 41. Spence, H. J., Chen, Y. J., and Winder, S. J. (2002) *Bioessays* **24**, 542–552
 42. Schwander, M., Leu, M., Stumm, M., Dorchies, O. M., Ruegg, U. T., Schittny, J., and Muller, U. (2003) *Dev. Cell* **4**, 673–685
 43. Allikian, M. J., Hack, A. A., Mewborn, S., Mayer, U., and McNally, E. M. (2004) *J. Cell Sci.* **117**, 3821–3830
 44. Allen, D. L., Teitelbaum, D. H., and Kurachi, K. (2003) *Am. J. Physiol.* **284**, C805–C815
 45. Ito, H., Duxbury, M., Benoit, E., Farivar, R. S., Gardner-Thorpe, J., Zinner, M. J., Ashley, S. W., and Whang, E. E. (2004) *Biochem. Biophys. Res. Commun.* **318**, 594–600
 46. Dee, K., Freer, M., Mei, Y., and Weyman, C. M. (2002) *Cell Death Differ.* **9**, 209–218
 47. Walsh, K., and Perlman, H. (1997) *Curr. Opin. Genet. Dev.* **7**, 597–602
 48. Yoshida, N., Yoshida, S., Koishi, K., Masuda, K., and Nabeshima, Y. (1998) *J. Cell Sci.* **111**, 769–779
 49. Beauchamp, J. R., Heslop, L., Yu, D. S. W., Tajbakhsh, S., Kelly, R. G., Wernig, A., Buckingham, M. E., Partridge, T. A., and Zammit, P. S. (2000) *J. Cell Biol.* **151**, 1221–1234
 50. Carnac, G., Fajas, L., L'honore, A., Sardet, C., Lamb, N. J., and Fernandez, A. (2000) *Curr. Biol.* **10**, 543–546
 51. Friday, B. B., and Pavlath, G. K. (2001) *J. Cell Sci.* **114**, 303–310
 52. Lawlor, M. A., Feng, X., Everding, D. R., Sieger, K., Stewart, C. E., and Rotwein, P. (2000) *Mol. Cell. Biol.* **20**, 3256–3265
 53. Jones, N. C., Fedorov, Y. V., Rosenthal, R. S., and Olwin, B. B. (2001) *J. Cell. Physiol.* **186**, 104–115
 54. Ostrovsky, O., and Bengal, E. (2003) *J. Biol. Chem.* **278**, 21221–21231
 55. Sorci, G., Riuzzi, F., Agneletti, A. L., Marchetti, C., and Donato, R. (2004) *J. Cell. Physiol.* **199**, 274–283
 56. Huttunen, H. J., Kuja-Panula, J., Sorci, G., Agneletti, A. L., Donato, R., and Rauvala, H. (2000) *J. Biol. Chem.* **275**, 40096–40105
 57. Yonekura, H., Yamamoto, Y., Sakurai, S., Petrova, R. G., Abedin, M. J., Li, H., Yasui, K., Takeuchi, M., Makita, Z., Takasawa, S., Okamoto, H., Watanabe, T., and Yamamoto, H. (2003) *Biochem. J.* **370**, 1097–1109

The Amphoterin (HMGB1)/Receptor for Advanced Glycation End Products (RAGE) Pair Modulates Myoblast Proliferation, Apoptosis, Adhesiveness, Migration, and Invasiveness: FUNCTIONAL INACTIVATION OF RAGE IN L6 MYOBLASTS RESULTS IN TUMOR FORMATION IN VIVO

Francesca Riuzzi, Guglielmo Sorci and Rosario Donato

J. Biol. Chem. 2006, 281:8242-8253.

doi: 10.1074/jbc.M509436200 originally published online January 9, 2006

Access the most updated version of this article at doi: [10.1074/jbc.M509436200](https://doi.org/10.1074/jbc.M509436200)

Alerts:

- [When this article is cited](#)
- [When a correction for this article is posted](#)

[Click here](#) to choose from all of JBC's e-mail alerts

This article cites 57 references, 31 of which can be accessed free at <http://www.jbc.org/content/281/12/8242.full.html#ref-list-1>